DOI:10.1093/jnci/djs373
Advance Access publication September 20, 2012
©The Author 2012. Published by Oxford University Press.
This is an Open Access article distributed under the terms of the Creative Commons Attribution Non-Commercial License (http://creativecommons.org/licenses/by-nc/3.0/), which permits unrestricted non-commercial use, distribution, and reproduction in any medium, provided the original work is properly cited.

BRIEF COMMUNICATION

Dual Suppression of the Cyclin-Dependent Kinase Inhibitors CDKN2C and CDKN1A in Human Melanoma

Ahmad Jalili, Christine Wagner, Mikhail Pashenkov, Gaurav Pathria, Kirsten D. Mertz, Hans R. Widlund, Mathieu Lupien, Jean- Philippe Brunet, Todd R. Golub, Georg Stingl, David E. Fisher, Sridhar Ramaswamy, Stephan N. Wagner

Manuscript received March 3, 2012; revised July 18, 2012; accepted July 24, 2012.

Correspondence to: Stephan N. Wagner, MD, Division of Immunology, Allergy and Infectious Diseases, Department of Dermatology, Medical University of Vienna, Waehringer Guertel 18-20, A-1090 Vienna, Austria (e-mail: stephan.wagner@meduniwien.ac.at).

Resistance to BRAF^{V600E} inhibitors is associated with reactivation of mitogen-activated protein kinase (MAPK) signaling at different levels in melanoma. To identify downstream effectors of MAPK signaling that could be used as potential additional therapeutic targets for BRAF^{V600E} inhibitors, we used hTERT/CDK4R24C/p53DD-immortalized primary human melanocytes genetically modified to ectopically express *BRAFV600E* or *NRASG12D* and observed induction of the AP-1 transcription factor family member c-Jun. Using a dominant negative approach, in vitro cell proliferation assays, western blots, and flow cytometry showed that MAPK signaling via BRAF^{V600E} promotes melanoma cell proliferation at G1 through AP-1-mediated negative regulation of the INK4 family member, cyclin-dependent kinase inhibitor 2C (CDKN2C), and the CIP/KIP family member, cyclin-dependent kinase inhibitor 1A (CDKN1A). These effects were antagonized by pharmacological inhibition of CDKN2C and CDKN1A targets CDK2 and CDK4 in vitro. In contrast to *BRAFV600E* or *NRASG12D*-expressing melanocytes, melanoma cells have an inherent resistance to suppression of AP-1 activity by BRAF^{V600E}- or MEK-inhibitors. Here, CDK2/4 inhibition statistically significantly augmented the effects of BRAF^{V600E}- or MEK-inhibitors on melanoma cell viability in vitro and growth in athymic nude *Foxn1^{nu}* mice (*P* = .03 when mean tumor volume at day 13 was compared for BRAF^{V600E} inhibitor vs BRAF^{V600E} inhibitor plus CDK2/4 inhibition; *P* = .02 when mean tumor volume was compared for MEK inhibitor vs MEK inhibitor plus CDK2/4 inhibition; *P* values were calculated by a two-sided Welch *t* test; n = 4–8 mice per group).

J Natl Cancer Inst 2012;104:1673–1679

Melanoma responses to BRAF^{V600E} inhibition (1,2) are often followed by disease recurrence through reactivation of the mitogen-activated protein kinase (MAPK) pathway (3), a nonlinear dynamic regulatory network of protein kinases (4). Resistance to BRAF^{V600E} inhibition occurs at different levels of this network, eg, through acquisition of new activating mechanisms such as mutations in NRAS or MEK (5,6), MEK kinase activation and CRAF overexpression (7), activation of alternative wild-type RAF heterodimers (8), or activation of platelet-derived growth factor receptor β (5) and insulin-like growth factor 1 receptor via functional cross-talk (8). Thus, we hypothesized that inhibition of downstream effectors of MAPK signaling could be a potential therapeutic strategy for BRAF^{V600E} inhibitor-resistant melanomas. To our knowledge, this therapeutic strategy has not been explored for melanoma.

To identify downstream effectors of MAPK signaling that could be used as potential therapeutic targets, we used hTERT/CDK4R24C/p53DD-immortalized primary human melanocytes genetically modified to ectopically express *BRAF^{V600E}* or *NRAS^{G12D}* (9). Protein lysates were subjected to western blot for activated and total c-Jun, an oncogenic subunit of the AP-1 transcription factor (Supplementary Methods, available online). AP-1 is a homo/heterodimeric transcription factor composed of c-Jun and JunD homo- or heterodimers, or heterodimers with other basic leucine-zipper family members (10), and is a major transducer of cellular proproliferative signals (10,11). We found that ectopic expression of *BRAF^{V600E}* or *NRAS^{G12D}* increased activation of c-Jun relative to parental hTERT/CDK4R24C/p53DD cells (Figure 1, A). Furthermore, when the cells were treated with the MEK1/2 inhibitor PD98059 (12) (Selleck Chemicals, Houston, TX), AP-1 activity was markedly decreased compared with untreated and solvent (control)-treated cells as detected by an AP-1-secreted alkaline phosphatase reporter gene assay (Supplementary Methods, available online).

To determine the effect of c-Jun knockdown on MAPK signaling in human melanoma cells, LOXIMVI cells were transiently transfected with three different small interfering RNAs (siRNAs) targeting c-Jun (Supplementary Methods, available online). After 48 hours, c-Jun knockdown was confirmed by western blot, and siRNA #145018 was used for all subsequent experiments (data not shown). siRNA transfected-LOXIMVI cells had decreased AP-1 activity relative to cells transfected with a nontarget control siRNA (mean AP-1 activity = 65.2%, SD = 18.4% vs 100%, SD = 7.0%, two-sided *P* = .07) (Supplementary Figure 1, A, available online). c-Jun knockdown also increased the percentage of cells in G1 compared with the nontarget control siRNA (21.5% vs 12.1%, data from one representative experiment), whereas the percentage of cells in S and G2M remained similar (Supplementary Methods, available online). Cell proliferation of c-Jun siRNA transfected cells was also decreased compared with nontarget siRNA transfected cells (mean cell number on day 4 = 8.6×10^3, SD = 0.2×10^3 vs 24.9×10^3, SD = 2.9×10^3, respectively, two-sided *P* = .01) (Supplementary Methods and Supplementary Figure 1, B, available online).

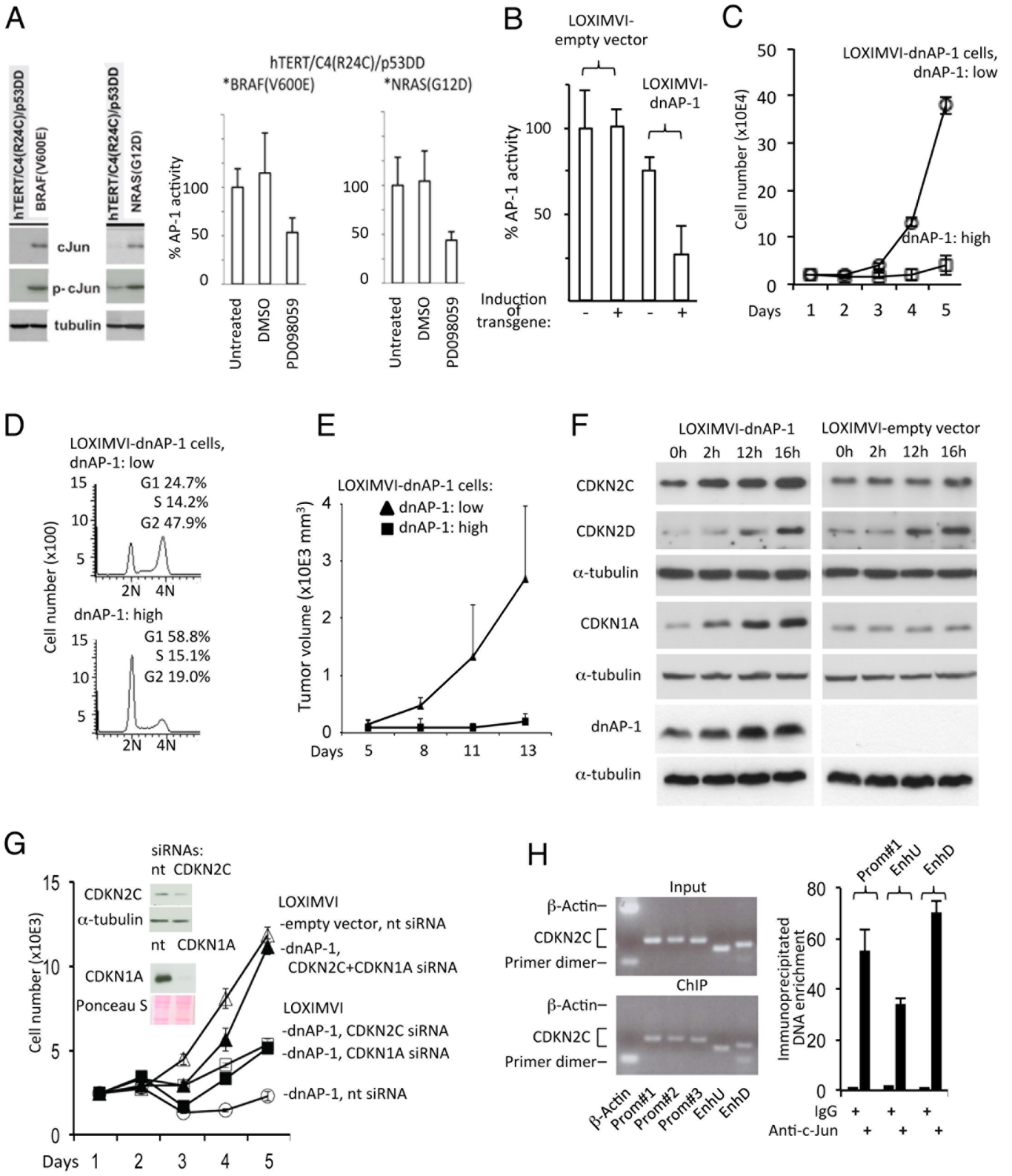

Figure 1. Mitogen-activated protein kinase, AP-1 activity, and proliferation of human melanocytic cells. **A**) Results of western blots for c-Jun and phosphorylated c-Jun (p-cJun) protein expression levels in primary immortalized human melanocytes (hTERT/C4(R24C)/p53DD) with or without ectopic expression of a $BRAF^{V600E}$ or $NRAS^{G12D}$ are shown (**left panel**). AP-1 activity in these cells was measured by AP-1-secreted alkaline phosphatase reporter gene assay after treatment with the MEK inhibitor PD098059 (50 μM) or dimethyl sulfoxide (**right panel**). Untreated cells served as an additional control. Results are representative of two independent experiments performed in triplicate. **B**) AP-1 activity was also measured in the NCI-60 $BRAF^{V600E}$ human melanoma LOXIMVI cell line, stably expressing dominant negative AP-1 and a puromycin resistance gene (-dnAP-1) or the resistance gene alone (-empty vector) with (0.75 μg/mL puromycin) and without induction (0.25 μg/mL puromycin) of the transgene for 48 hours. **Whisker bars** indicate the SD. Results are representative of three independent experiments performed in triplicate. **C**) Cell proliferation of LOXIMVI-dnAP-1 cells upon induction of dnAP-1 as determined by cell numbers over time. The means and corresponding SD (**whisker bars**) of

Transfection of the LOXIMVI melanoma cell line with a dominant negative c-Jun mutant (dnAP-1), which leads to a broader inhibition of AP-1 activity by binding additional AP-1 members compared with c-Jun siRNA (13), was done with the bicistronic pIRESpuro3 vector (Clontech Laboratories, Mountain View, CA) to stably express a puromycin resistance gene with or without a FLAG-tagged dnAP-1 (14) (referred to hereafter as -dnAP-1 and -empty vector cells, respectively). When cultured in a low concentration of puromycin (0.25 μg/mL), LOXIMVI-dnAP-1 cells expressed low levels of the resistance gene and dnAP-1 without an impact on AP-1 activity (Figure 1, B), cell proliferation, or cell cycle distribution (data not shown) compared with LOXIMVI-empty-vector cells. When cultured at a high concentration of puromycin (0.75 μg/mL), LOXIMVI-dnAP-1 cells expressed high levels of dnAP-1 in the cytoplasm and the nucleus (Supplementary Figure 1, C and D, available online) and showed decreased AP-1 activity (mean AP-1 activity = 26.5%, SD = 16.5% vs 75.3%, SD = 8.3%, respectively, two-sided $P = .02$) (Figure 1, B), decreased cell proliferation (mean cell number at day 5 = 4.1 x 10^4, SD = 0.2 x 10^4 vs 37.9 x 10^4, SD = 0.6 x 10^4, respectively, two-sided $P < .001$) (Figure 1, C), accumulation of cells in G1 (Figure 1, D), and decreased [^{3}H]thymidine uptake (data not shown) compared with culturing at a low concentration of puromycin.

To investigate the effect of AP-1 inhibition in melanoma cells in vivo, 1 x 10^6 LOXIMVI-dnAP-1 cells were injected subcutaneously into female, 6–8-week-old, athymic nude *Foxn1*^{nu} mice (Supplementary Methods, available online). Animal care procedures followed the guidelines of the Animal Research Committee of the Medical University of Vienna. Injection of LOXIMVI-dnAP-1 xenografts with 0.75 μg/mL puromycin every other day inhibited tumor growth compared with xenografts injected with 0.25 μg/mL puromycin (Figure 1, E), indicating that AP-1 activity is required for in vivo growth of human melanoma cells.

Because the effects of induced expression of dnAP-1 on cell proliferation (by counting cell numbers over time, Figure 1, C and Supplementary Figure 1, E, available online) and cell cycle distribution (not shown) were similar in human UACC257 melanoma cells and LOXIMVI cells that are cyclin-dependent kinase inhibitor CDKN2A–deficient, we investigated the effect of dnAP-1 on the expression of other cell cycle regulators at G1 by western blot. We found that CDKN2C and CDKN1A protein levels in LOXIMVI-dnAP-1 cells were increased relative to LOXIMVI empty vector cells within 2 hours of induction of dnAP-1 with puromycin (Figure 1, F). CDKN2D, CCND1, and CDK6 protein levels increased later at 12 and 16 hours after dnAP-1 induction in both LOXIMVI-dnAP-1 and LOXIMVI-empty vector cells. CDK2 and CDK4 protein levels remained almost unchanged within 24 hours (Figure 1, F and Supplementary Figure 1, F, available online). In addition, we observed nuclear and cytoplasmic accumulation of CDKN2C and nuclear accumulation of CDKN1A by immunofluorescence in LOXIMVI-dnAP-1 cells 48 hours after induction of dnAP-1 using puromycin (Supplementary Figure 1, G and H, available online).

Consistent with these findings, transfection of LOXIMVI cells with siRNA targeting CDKN2C or CDKN1A in vitro partially rescued dn-AP1-induced suppression of cell proliferation, and when both CDKN2C and CDKN1A siRNAs were cotransfected into LOXIMVI cells, cell proliferation (as measured by counting cell numbers over time, which is shown in Figure 1, G, and [^{3}H]thymidine uptake [data not shown]) was similar to that of LOXIMVI-empty vector control cells. Similar effects were not seen when siRNA targeting other cell cycle regulators (TP53, CDKN1B, CDKN1C alone or in combination with CDKN2C) was used (data not shown). These results indicate that the full proproliferative effect of AP-1 on melanoma cells requires suppression of both the INK4 family member CDKN2C and the CIP/KIP family member CDKN1A. This finding supports a previous report in which the ability of CDK4^{R24C} (an INK4-insensitive CDK4 mutant) to rescue *Cdkn1a*$^{-/-}$ but not *Cdkn1a*^{wt} cells from growth arrest (15), an important prerequisite for cell transformation, was described. Furthermore, mutations in *CDK4* have been described in melanoma-prone families and patients with multiple primary melanomas (16), *CDK4* amplification has been previously reported in subtypes of sporadic melanoma (17), and reduced CDKN1A expression has been implicated in melanoma metastasis (18).

As AP-1 is a transcription factor, we performed cotransfection assays with wild-type *CDKN2C* and *CDKN1A* promoter-luciferase reporter plasmids (19,20) in LOXIMVI-dnAP-1 and LOXIMVI-empty vector cells. When cultured at a high concentration of puromycin (0.75 μg/mL) for 4 hours, LOXIMVI-dnAP-1 cells showed activated expression from both promoter reporter plasmids compared with LOXIMVI-empty vector cells (mean fold CDKN2C promoter

Figure 1. (Continued)

a representative experiment performed in triplicate are shown. Four independent experiments were performed with similar results. **D**) Cell cycle analysis was performed by flow cytometry of propidium iodide–stained LOXIMVI-dnAP-1 cells 48 hours after induction of dnAP-1 with a high concentration (0.75 μg/mL) of puromycin and compared with LOXIMVI-dnAP-1 cells exposed to a low concentration (0.25 μg/mL) of puromycin. The percentages of cells in G1, S, and G2 phases of the cell cycle are shown. **E**) In vivo growth of LOXIMVI-dnAP-1 cells was measured in athymic nude *Foxn1*^{nu} mice (n = 6 mice per group) with or without induction of dnAP-1 by injection of 50 μL of low (0.25 μg/mL) or high (0.75 μg/mL) concentrations of puromycin in phosphate buffered saline every other day. **Whisker bars** indicate the upper SD. **F**) Western blot of cell lysates with anti-CDKN2C, dnAP-1/c-Jun, CDKN2D, CDKN1A, α-tubulin antibodies of LOXIMVI-dnAP-1 and -empty vector cells was done at 0, 2, 12, and 16 hours after induction of dnAP-1. This experiment was performed three times with similar results. **G**) Cell proliferation was determined by counting LOXIMVI-dnAP-1 cell numbers after induction of dnAP-1 and transfection with small interfering RNAs (siRNAs) targeting CDKN2C, CDKN1A, or CDKN1A and CDKN2C. As a reference, LOXIMVI-empty vector cells were treated with nontarget small interfering RNA (nt siRNA). siRNA transfection was confirmed by western blot (**inset**). The means with SD (**whisker bars**) are given. Results are representative of three independent experiments performed in triplicate. **H**) Chromatin immunoprecipitation assay of LOXIMVI cells was done with anti-c-Jun antibody and polymerase chain reaction primer sets for the *β-ACTIN* and *CDKN2C* promoters (Prom#1, #2, and #3) and enhancer (EnhU and EnhD) regions (**left panel**). Quantitative polymerase chain reaction signals for Prom#1, EnhU, and EnhD regions were normalized to the input and expressed as the mean with SD (**whisker bars**). As a control, the anti-c-Jun antibody was substituted with IgG (**right panel**). The results are representative of two independent experiments.

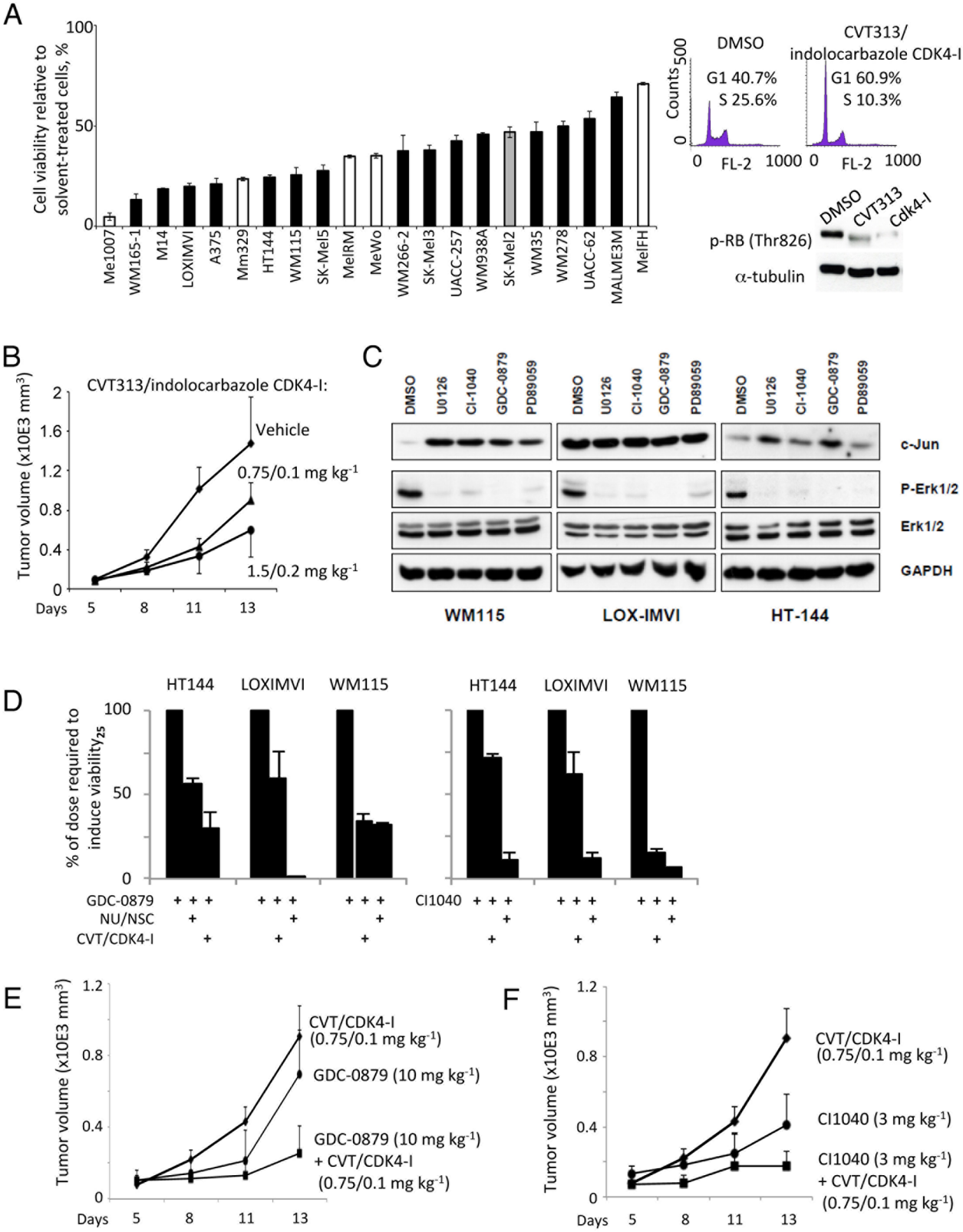

Figure 2. Melanoma cell viability and in vivo growth by cyclin-dependent kinase 2/4 inhibition. **A**) Cell viability was assessed by 3-(4,5-dimethylthiazol-2-yl)-2,5-diphenyltetrazolium-bromide assay of human melanoma cell lines (**white**, **gray**, and **black bars** indicate *BRAF*^{wt}/*NRAS*^{wt}, *NRAS*^{Q61R}, and *BRAF*^{V600E} cell lines, respectively) treated with a CDK2/4 inhibitor combination (2 μM CVT313 plus 0.25 μM indolocarbazole CDK4-I) for 48 hours. The values are presented as the percentage of treatment with dimethyl sulfoxide (DMSO, solvent). **Whisker bars** indicate the SD (**left panel**). On-target effects of CDK2/4 inhibitors in LOXIMVI cells are shown in the right panel: cell cycle analysis by flow cytometry was done after treatment with DMSO (solvent) control or the CVT313/indolocarbazole CDK4-I combination for 12 hours; western blot analysis was also done to detect phosphorylated retinoblastoma (p-RB) (Thr826) levels after treatment with DMSO (solvent) control, 2 μM CVT313, or 0.25 μM indolocarbazole CDK4-I for 48 hours. These experiments were performed three

induction for LOXIMVI-dnAP-1 cells vs LOXIMVI-empty vector cells = 3.1, SD = 0.2 vs 1.0, SD = 0.02, two-sided P = .002; mean fold CDKN1A promoter induction for LOXIMVI-dnAP-1 cells vs LOXIMVI-empty vector cells = 1.7, SD = 0.1 vs 1, SD = 0.1, two-sided P < .001) (Supplementary Methods and Supplementary Figure 2, A, available online), further supporting the link between AP-1 activity and *CDKN2C* and *CDKN1A* expression. As dn-AP-1 induced CDKN2C mRNA in LOXIMVI-dnAP-1 cells (by quantitative reverse transcription-real time PCR, data not shown) independent of protein synthesis (by cycloheximide, data not shown), we performed chromatin immunoprecipitation from LOXIMVI cells with an anti-c-Jun antibody followed by polymerase chain reaction using primer sets spanning putative AP-1-binding sites at the *CDKN2C* gene (21) (Supplementary Methods, available online). We observed binding of AP-1 at two promoter-distant regions upstream and downstream of *CDKN2C*, each harboring a 12-*O*-tetradecanoate-13-acetate response element-binding motif, and one region within the promoter (Figure 1, H). These results indicate that *CDKN2C* is a direct target of AP-1.

In addition, we assessed the relationship between c-Jun expression and that of CDKN2C and CDKN1A using RNA and tissues obtained from 30 melanoma patients. The primary human melanomas were assigned to two groups (low and high) based on low vs high expression of CDKN2C and CDKN1A (mean relative CDKN2C mRNA expression = 0.5, SD = 0.3 vs 2.5, SD = 1.8, respectively, two-sided P = .007; mean relative CDKN1A mRNA expression = 0.9, SD = 0.4 vs 3.0, SD = 1.2, respectively, two-sided P < .001; n = 8 and 11, respectively) as determined by quantitative real-time PCR of available RNA (Supplementary Methods, available online). Nuclear phospho-c-Jun expression in the corresponding tissues was then analyzed by immunohistochemistry (Supplementary Methods, available online), and the percentage of cells with 0–1+, 2+, and 3+ staining was determined. A table summarizing the data and representative stained tissues are depicted in Supplementary Figure 2, B (available online). High levels of CDKN2C and CDKN1A mRNA were associated with low phospho-c-Jun staining (0–1+), whereas low levels of CDKN2C and CDKN1A mRNA were associated with high phospho-c-Jun staining (2+ and 3+). These results further substantiate the role of AP-1 in the negative regulation of CDKN2C and CDKN1A transcription. In accordance with these results, previous studies in animal models have shown that $CDK4^{R24C}$ and a CDKN2C deficiency increase melanoma susceptibility, but additional MAPK signaling is required for melanomas to develop (22,23).

Because the expression of CDKN2C and CDKN1A targets, ie, CDK2 and CDK4/6, was unaffected by dnAP-1 (Supplementary Figure 1, F, available online) and is rarely lost in human melanoma (24), our results provide rationale for the development of novel combination therapeutic strategies for melanoma. In contrast to single agent-treatment with inhibitors at doses selective to CDK2 or CDK4 inhibition [NU6140 (25), CVT-313 (26), NSC625987 (27), indolocarbazole CDK4-I (28)] (Supplementary Methods and Supplementary Figure 2, C, available online), the combination of CDK2/4 inhibitors reduced viability in a panel of melanoma cell lines (by 3-[4,5-dimethylthiazol-2-yl]-2,5-diphenyltetrazolium-bromide assay) (Figure 2, A) and statistically significantly the growth of LOXIMVI xenografts in vivo (mean tumor volume at day 13: vehicle only = 1.5 x 10^3 mm^3, SD = 0.5 x 10^3 mm^3; 0.75/0.1 mg/kg dose level = 0.9 x 10^3 mm^3, SD = 0.2 x 10^3 mm^3; 1.5/0.2 mg/kg dose level = 0.6 x 10^3 mm^3, SD = 0.3 x 10^3 mm^3; vehicle vs 0.75/0.1 mg/kg dose, two-sided P = .05; vehicle vs 1.5/0.2 mg/kg dose, two-sided P = .01; n = 6–8 mice per group) (Figure 2, B). Reduction of viability was independent of the presence or absence of $BRAF^{V600E}$/$NRAS^{Q61R}$ as were nuclear phospho-c-Jun and CDKN2C/CDKN1A transcript levels in primary melanomas. Furthermore, in $BRAF^{V600E}$ melanoma cells, the highly selective $BRAF^{V600E}$ inhibitor GDC-0879 (29) and three selective MEK inhibitors [PD184352/CI-1040 (30), U0126 (31), PD98059 (12)] did not suppress c-Jun levels, although they effectively reduced phospho-ERK levels (Figure 2, C). Together these data suggest that in melanoma cells, in contrast to melanocytes, pathways that bypass the BRAF-MEK-ERK axis to induce AP-1 are operative. Consistent with this hypothesis, AP-1 and CDK2/4 inhibition increased the magnitude of the reduction of melanoma cell viability/proliferation by $BRAF^{V600E}$ inhibitor GDC-0879 and MEK inhibitor PD184352/CI1040 in vitro (Figure 2, D and Supplementary Figure 2, D, available

Figure 2. (Continued)

times with similar results. **B**) In vivo growth of LOXIMVI xenograft tumors in athymic nude *Foxn1*^{nu} mice systemically treated with the CDK2/4 inhibitor combination (CVT-313 plus indolocarbazole CDK4-I) is shown. Growth reduction was observed by comparison of vehicle only vs 0.75/0.1 mg/kg (P = .05) and 1.5/0.2 mg/kg (P = .01) dose levels (n = 6–8 mice per group, two-sided Welch's t test was used to calculate P). **Whisker bars** indicate the upper or lower SD. **C**) Western blot analysis for c-Jun, phosphorylated-ERK1/2 (Thr202/Tyr204) (p-ERK1/2), and total ERK1/2 protein levels was done for human melanoma cell lines treated with the $BRAF^{V600E}$ inhibitor GDC-0879 (1 μM), or MEK inhibitors CI-1040 (1 μM), U0126 (1 μM), and PD98059 (10 μM) for 18 hours. Glyceraldehyde 3-phosphatase dehydrogenase (GAPDH) was used as the loading control. This experiment was performed three times with similar results. **D**) Cell viability of HT144, LOXIMVI, and WM115 human melanoma cell lines after exposure to different combinations of CDK2/4 with MEK- and $BRAF^{V600E}$-inhibitors was assessed by 3-(4,5-dimethylthiazol-2-yl)-2,5-diphenyltetrazolium-bromide assay after 72 hours. Simultaneous treatment with the indicated CDK2/4 inhibitor combinations [NU6140 (2 μM) plus NSC625987 (20 μM) or CVT-313 (2 μM) plus indolocarbazole CDK4-I (0.25 μM)] decreased the dose of MEK- and $BRAF^{V600E}$-inhibitors required to reduce melanoma cell viability by 75% ($viability_{25}$). **Whisker bars** indicate the SD. Results are representative of four independent experiments performed in triplicates. **E** and **F**) In vivo growth of LOXIMVI xenografts in athymic nude *Foxn1*^{nu} mice is shown. Tumors were allowed to grow to a maximum volume of 250 mm^3, and the mice were subsequently treated daily at the indicated dose levels with CDK2/4 inhibitors by intraperitoneal injection in combination with a $BRAF^{V600E}$- or MEK-inhibitor. **E**) CDK2/4 inhibitor (CVT-313/indolocarbazole CDK4-I) treatment sensitizes tumors to systemic treatment with $BRAF^{V600E}$ inhibitor GDC-0879 (GDC-0879 vs GDC-0879 plus CVT-313/indolocarbazole CDK4-I: P = .03, n = 5–8 per group, two-sided Welch's t test). **F**) CDK2/4 inhibitor (CVT-313/indolocarbazole CDK4-I) treatment sensitized tumors to systemic treatment with MEK-inhibitor CI1040 (CI1040 vs CI1040 plus CVT-313/indolocarbazole CDK4-I; P = .02, n = 4–8 per group, two-sided Welch's t test). **Whisker bars** indicate the upper SD.

online), and CDK2/4 inhibition augmented statistically significant growth reduction of melanoma xenografts in vivo by the BRAF and MEK inhibitors (P = .03 when mean tumor volume at day 13 was compared for GDC-0879 vs GDC-0879 plus CDK2/4 inhibition; P = .02 when mean tumor volume was compared for PD184352/CI1040 vs PD184352/CI1040 plus CDK2/4 inhibition; n = 4–8 mice per group) (mean tumor volume at day 13: GDC-0879 = 0.7 x 10^3 mm^3, SD = 0.2 x 10^3 mm^3; GDC-0879 plus CDK2/4 inhibition = 0.3 x 10^3 mm^3, SD = 0.2 x 10^3 mm^3; GDC-0879 vs GDC-0879 plus CDK2/4 inhibition, two-sided P = .03; PD184352/CI1040 = 0.4 x 10^3 mm^3, SD = 0.2 x 10^3 mm^3; PD184352/CI1040 plus CDK2/4 inhibition = 0.2 x 10^3 mm^3, SD = 0.1 x 10^3 mm^3; PD184352/CI1040 vs PD184352/CI1040 plus CDK2/4 inhibition, two sided P = .02; n = 4–8 mice per group) (Figure 2, E and F).

Our study was not without limitations. The restricted ability of cell-based studies to predict clinical behavior is an inherent restraint. Also, the varied response to cyclin-dependent kinase inhibitors between different melanoma cell lines is unexplained at this time. The small number of available human tissue samples used in our study also limits the interpretation of our results.

Nevertheless, our data show a statistically significant augmentation of $BRAF^{V600E}$- and MEK-inhibitors by CDK2/4 inhibition in vivo. Our findings provide rationale and support for further clinical exploration of this novel combination therapeutic strategy for melanoma.

References

1. Chapman PB, Hauschild A, Robert C, et al.; BRIM-3 Study Group. Improved survival with vemurafenib in melanoma with BRAF V600E mutation. *N Engl J Med*. 2011;364(26):2507–2516.
2. Flaherty KT, Puzanov I, Kim KB, et al. Inhibition of mutated, activated BRAF in metastatic melanoma. *N Engl J Med*. 2010;363(9):809–819.
3. Bollag G, Hirth P, Tsai J, et al. Clinical efficacy of a RAF inhibitor needs broad target blockade in BRAF-mutant melanoma. *Nature*. 2010;467(7315):596–599.
4. Cuevas BD, Abell AN, Johnson GL. Role of mitogen-activated protein kinase kinase kinases in signal integration. *Oncogene*. 2007;26(22):3159–3171.
5. Nazarian R, Shi H, Wang Q, et al. Melanomas acquire resistance to B-RAF(V600E) inhibition by RTK or N-RAS upregulation. *Nature*. 2010;468(7326):973–977.
6. Wagle N, Emery C, Berger MF, et al. Dissecting therapeutic resistance to RAF inhibition in melanoma by tumor genomic profiling. *J Clin Oncol*. 2011;29(22):3085–3096.
7. Johannessen CM, Boehm JS, Kim SY, et al. COT drives resistance to RAF inhibition through MAP kinase pathway reactivation. *Nature*. 2010;468(7326):968–972.
8. Villanueva J, Vultur A, Lee JT, et al. Acquired resistance to BRAF inhibitors mediated by a RAF kinase switch in melanoma can be overcome by cotargeting MEK and IGF-1R/PI3K. *Cancer Cell*. 2010;18(6):683–695.
9. Jané-Valbuena J, Widlund HR, Perner S, et al. An oncogenic role for ETV1 in melanoma. *Cancer Res*. 2010;70(5):2075–2084.
10. Eferl R, Wagner EF. AP-1: a double-edged sword in tumorigenesis. *Nat Rev Cancer*. 2003;3(11):859–868.
11. Lopez-Bergami P, Huang C, Goydos JS, et al. Rewired ERK-JNK signaling pathways in melanoma. *Cancer Cell*. 2007;11(5):447–460.
12. Dudley DT, Pang L, Decker SJ, Bridges AJ, Saltiel AR. A synthetic inhibitor of the mitogen-activated protein kinase cascade. *Proc Natl Acad Sci U S A*. 1995;92(17):7686–7689.
13. Ham J, Babij C, Whitfield J, et al. A c-Jun dominant negative mutant protects sympathetic neurons against programmed cell death. *Neuron*. 1995;14(5):927–939.
14. Hennigan RF, Stambrook PJ. Dominant negative c-jun inhibits activation of the cyclin D1 and cyclin E kinase complexes. *Mol Biol Cell*. 2001;12(8):2352–2363.
15. Quereda V, Martinalbo J, Dubus P, Carnero A, Malumbres M. Genetic cooperation between p21Cip1 and INK4 inhibitors in cellular senescence and tumor suppression. *Oncogene*. 2007;26(55):7665–7674.
16. Holland EA, Schmid H, Kefford RF, Mann GJ. CDKN2A (P16(INK4a)) and CDK4 mutation analysis in 131 Australian melanoma probands: effect of family history and multiple primary melanomas. *Genes Chromosomes Cancer*. 1999;25(4):339–348.
17. Curtin JA, Fridlyand J, Kageshita T, et al. Distinct sets of genetic alterations in melanoma. *N Engl J Med*. 2005;353(20):2135–2147.
18. Maelandsmo GM, Holm R, Fodstad O, Kerbel RS, Flørenes VA. Cyclin kinase inhibitor p21WAF1/CIP1 in malignant melanoma: reduced expression in metastatic lesions. *Am J Pathol*. 1996;149(6):1813–1822.
19. Carreira S, Goodall J, Aksan I, et al. Mitf cooperates with Rb1 and activates p21Cip1 expression to regulate cell cycle progression. *Nature*. 2005;433(7027):764–769.
20. Matsuzaki Y, Takaoka Y, Hitomi T, Nishino H, Sakai T. Activation of protein kinase C promotes human cancer cell growth through downregulation of p18(INK4c). *Oncogene*. 2004;23(31):5409–5414.
21. Carroll JS, Meyer CA, Song J, et al. Genome-wide analysis of estrogen receptor binding sites. *Nat Genet*. 2006;38(11):1289–1297.
22. Sotillo R, García JF, Ortega S, et al. Invasive melanoma in Cdk4-targeted mice. *Proc Natl Acad Sci USA*. 2001;98(23):13312–13317.
23. Hacker E, Muller HK, Irwin N, et al. Spontaneous and UV radiation-induced multiple metastatic melanomas in Cdk4R24C/R24C/TPras mice. *Cancer Res*. 2006;66(6):2946–2952.
24. Halaban R, Cheng E, Zhang Y, Mandigo CE, Miglarese MR. Release of cell cycle constraints in mouse melanocytes by overexpressed mutant E2F1E132, but not by deletion of p16INK4A or p21WAF1/CIP1. *Oncogene*. 1998;16(19):2489–2501.
25. Pennati M, Campbell AJ, Curto M, et al. Potentiation of paclitaxel-induced apoptosis by the novel cyclin-dependent kinase inhibitor NU6140: a possible role for survivin down-regulation. *Mol Cancer Ther*. 2005;4(9):1328–1337.
26. Brooks EE, Gray NS, Joly A, et al. CVT-313, a specific and potent inhibitor of CDK2 that prevents neointimal proliferation. *J Biol Chem*. 1997;272(46):29207–29211.
27. Kubo A, Nakagawa K, Varma RK, et al. The p16 status of tumor cell lines identifies small molecule inhibitors specific for cyclin-dependent kinase 4. *Clin Cancer Res*. 1999;5(12):4279–4286.
28. Zhu G, Conner SE, Zhou X, et al. Synthesis, structure-activity relationship, and biological studies of indolocarbazoles as potent cyclin D1-CDK4 inhibitors. *J Med Chem*. 2003;46(11):2027–2030.
29. Hoeflich KP, Herter S, Tien J, et al. Antitumor efficacy of the novel RAF inhibitor GDC-0879 is predicted by BRAFV600E mutational status and sustained extracellular signal-regulated kinase/mitogen-activated protein kinase pathway suppression. *Cancer Res*. 2009;69(7):3042–3051.
30. Sebolt-Leopold JS, Dudley DT, Herrera R, et al. Blockade of the MAP kinase pathway suppresses growth of colon tumors in vivo. *Nat Med*. 1999;5(7):810–816.
31. Duncia JV, Santella JB III, Higley CA, et al. MEK inhibitors: the chemistry and biological activity of U0126, its analogs, and cyclization products. *Bioorg Med Chem Lett*. 1998;8(20):2839–2844.

Funding

The research was supported by the FWF-Austrian Science Fund (L590-B12 to SNW) and by a grant from the Austrian Society of Dermatology and Venerology (to AJ).

Notes

The funders did not have a role in the study design; data collection, analysis, or interpretation; the writing of the brief communication; or the decision to submit the brief communication for publication. T. R. Golub is a consultant of Merck-EMD Serono, Inc, Pfizer, Inc, and holds stocks/stock options with H3 Biomedicine.

Affiliations of authors: Division of Immunology, Allergy and Infectious Diseases, Department of Dermatology, Medical University of Vienna (AJ, CW, GP, KDM, GS, SNW) and CeMM-Research Center for Molecular Medicine of the Austrian

Academy of Sciences, Vienna, Austria (SNW); Laboratory of Clinical Immunology, National Research Center Institute of Immunology, Federal Medical and Biological Agency, Moscow, Russia (MP); Department of Pediatric Oncology, Dana-Farber Cancer Institute and Brigham and Women's Hospital and Department of Dermatology, Harvard Medical School, Boston, MA (HRW); Department of Genetics, Norris Cotton Cancer Center, Dartmouth Medical School, Lebanon, NH (ML); The Broad Institute of Harvard University and Massachusetts Institute of Technology, Cambridge, MA (JPB, TRG, SR); Department of Pediatric Oncology and Center for Genome Discovery, Dana-Farber Cancer Institute, Boston, MA (TRG); Howard Hughes Medical Institute, Chevy Chase, MD (TRG); Department of Dermatology, Cutaneous Biology Research Center, Melanoma Program in Medical Oncology, Harvard Medical School, Boston, MA (DEF); Massachusetts General Hospital Cancer Center, Boston, MA (SR); Harvard Stem Cell Institute, Cambridge, MA (SR).